PalArch's Journal of Archaeology of Egypt / Egyptology

FUZZY BASED VECTOR CONTROL METHOD FOR BLDC MOTOR DRIVE WITH FIVE-SWITCH THREE-PHASE TOPOLOGY

G Madhusudhana Rao,
Professor
Dept of ECE
Bule Hora University, Ethiopia

Ch Vinay Kumar,
Asst.Professor
Dept of EEE
MGIT, Hyd

A.RaghuRam
Professor
Dept of EEE
JNTUCEH, Hyd

G Madhusudhana Rao, Ch Vinay Kumar,A.RaghuRam, Fuzzy Based Vector Control Method for BLDC Motor Drive with Five-Switch Three-Phase Topology-Palarch's Journal Of Archaeology Of Egypt/Egyptology 17(12), ISSN 1567-214x

***Abstract*—**The Brushless DC Motor is a type of permanent magnetic motors which will be having high performance in recent years and replaced the Brushed DC Motors. The BLDC motors have higher efficiency and precise dynamic response increases in the Industrial applications. This paper proposed that the low cost design of the three phase Brushless DC Motor and it is analyzed with the vector control scheme. The working principle of the BLDC is with the help of five-switch control scheme can be implemented here. The proposed method is also reduces the current distortions where the frequency is varies with the speed and load. Later the current control is implemented with the Fuzzy logic control to maintain the accurate rating of the current. The fuzzy logic control scheme is implemented to reduce the current distortions and maintain the good speed. However the DC link of the five switching inverter is used here for the boosting of the voltage. The effectiveness of the Fuzzy based vector controlled method with the five-switch model is designed and implemented in Simulink/Mat lab

Key words: BLDC Motor, Current Distortions, Five-Switch, Inverter Topology, Vector Control, Fuzzy Logic Control

I. Introduction

Brushless DC motor (BLDCM) has been used widely in industrial applications and research works have been conducted in different aspects due to its advantages of high power density, high efficiency, easy maintenance, and so on [1]–[4]. Sensorless control technologies have been proposed for the BLDCM with the FSTP inverter, and the cost of the whole control system is reduced further by eliminating Hall-effect position sensors [5], [6]. In BLDCM drive with the conventional FSTP inverter, since the terminal of phase C winding is directly connected to the midpoints of capacitors on the side of power supply, three-phase currents are likely to be distorted by phase C back-EMF if a common bipolar switching modulation method is employed. Aiming at reducing possible current distortion caused by phase C back-EMF, different schemes have been proposed by scholars [6]–[10]. An asymmetric PWM scheme was proposed in [6] to reduce the influence of phase C back-EMF in Modes I and IV by turning all the switches OFF. A direct current control scheme was proposed in [7], where three-phase currents are controlled to be in quasi-square waveforms by controlling the currents of phases A and B independently with two hysteresis current controllers. DTC was used in FSTP BLDCM drives in [8], and with torque hysteresis controllers, distorted currents are reduced and smooth electromagnetic torque is produced by controlling the torques on phases A and B independently. A single current sensor-based control scheme was proposed in [9], where phase C current is maintained at nearly zero level in Modes I and IV by combining four sub operating modes according to different operational conditions. The schemes proposed for reducing current distortion caused by phase C back-EMF in [7]–[9] are all hysteresis control in nature, where switching frequency varies with load and speed and high control period of digital signal processor (DSP) is also necessary in order to obtain good performance. A three effective vectors-based current control scheme is proposed in [10], with constant frequency and small current ripple and good performance in speed. However, the utilization of dc link voltage with the FSTP inverter is only half of that with the SSTP inverter [6]–[10]. Therefore, in the cases of solar power and battery, where the voltage is lower than the rated voltage of motor the load and speed ranges of BLDCM are greatly restricted without independent boost unit [11].

6-Step Commutation with Current Control Method:

Since this configuration cannot control the current during fast torque reversal, it is only used when the direction of torque and speed are always identical during fast torque reversal condition. There may be chance of short circuit and also 6-step control produce high torque ripple. Especially during transition of commutation [17], [18] and the overall system has high audible noise and efficiency is poor.

For induction motors flux control has been developed, which offers a high dynamic performance for electric traction application. However this control type is complex and sophisticated. The development of BLDC has permitted by important simplification in the hardware for electric traction control. The term BLDC motor is used to identify the combination of AC machine, Solid State inverter and rotor position sensor that results in a drive system having a linear torque – speed characteristic as in conventional DC machine.

The two kind of Brushless [13] permanent magnet machine are used for traction application

- BLDC motor in which the air gap flux distribution and counter EMF, or back EMF waveform are approximately trapezoidal as like in conventional DC machine.
- Standard permanent magnet [14], [15] synchronous motor (PMSM) in which the air gap flux distribution and back EMF wave form are both sinusoidal is sometimes called as a Sinusoidal Brushless DC motor when operated in a self-controlled mode.

Indeed the drive characteristic and control methods are very similar for the trapezoidal and sinusoidal machines. In both cases, the motor must be energized with controlled currents that are synchronized with rotor position. However a distinction is now being drawn between the two drives, because of the differences in machine construction and the standard synchronous motor requires sinusoidal current excitation, whereas the trapezoidal machine is energized with square-wave and quasi-wave currents.

The rotor position sensors of the trapezoidal machine usually consist of a number of simple position detectors, such as Hall Effect devices that can sense rotor magnetic field and determine the phase switching points. The sinusoidal machine requires more precise position information to allow accurate synthesis of the sinusoidal current waveforms. Following are the significant of using brush less motor design;

- The position sensor system for the shaft is simple and needs only to deliver six digital signals for commanding the transistor of the inverter.
- The quasi square-wave armatures current are mainly characterized by their maximum amplitude value, which directly controls the machine torque.
- The inverter performance is very much reliable because there is natural dead time for each transistor.

The first and third characteristics allow reducing the complex circuitry required by other machine and allowing the self-synchronization process for the operation of the machine. The second characteristic allows designing a circuit [16] for controlling only a DC component which represents the maximum amplitude value of the trapezoidal current, I_{MAX}.

II. METHODOLOGY

This current control strategy [19] is developed and implemented on the MATLAB / Simulink version 7. It has many advantages over power electronic [20] circuit-oriented simulator (i.e., spice and its derivatives). Some of them are listed below

I) Fast and Accurate Simulation

The basic model of the switching device used in MATLAB / Simulink is a piece-wise linear model composed of a threshold voltage in series with a resistor. The resistor value varies with the switching state. It takes very high value (R_{off}>le6) in the turn-off state and a very small value (R_{on}<le-3) in the turn-on state. The transition between these two states takes place exponentially, if the transition time (turn-off time t_{off} and turn-on time t_{on}) is not zero. Modeling the power semiconductor devices as piece-wise linear switches instead of the complex physical models, leads to very fast and accurate simulation, without the risk of numerical instability [21].

II) Modeling of Linear, Nonlinear and Time Variant Components

Modeling of linear, non linear and time variant circuit [22] components is very easy with MATLAB/Simulink .MATLAB / Simulink automatically linearizes the complete electric circuit about the operating point. However the nonlinear electrical circuit component parameters should be defined as an element of the Simulink input vector u, allowing the component value to be dynamically defined by any Simulink block. The MATLAB / Simulink environment offers the possibility of partitioning large power electronics system (large system matrix) into many small systems (many small matrices), which can be modeled as separate S-function to facilitate accurate and fast simulation of large power electronics [23] systems including complex control systems. It is known that BLDC motor is driven by rectangular or trapezoidal voltage strokes coupled with given rotor position. The generated stator flux interacts with the rotor flux, which is generated by a rotor magnet, defines the torque and thus the speed of the motor. The voltage strokes must be properly applied to the two phases of the 3-phase winding system so that the angle between the stator flux and the rotor flux is kept close to 90º for the maximum generated torque. Eventually the motor is need of electronic control for proper operation. A standard 3-phase power inverter is used for common 3-phase BLDC motor. In self control mode, the inverter acts like an Electronic Commutator (ECM) that receives switching logic pulses from the absolute position sensor. The power inverter utilizes six power transistors. Fig 4.1 shows Inverter Circuit with BLDC Machine

Fundamentally inverter can be operated by the following two modes

- $2\pi/3$ angle switch on mode
- Voltage and current control PWM mode.

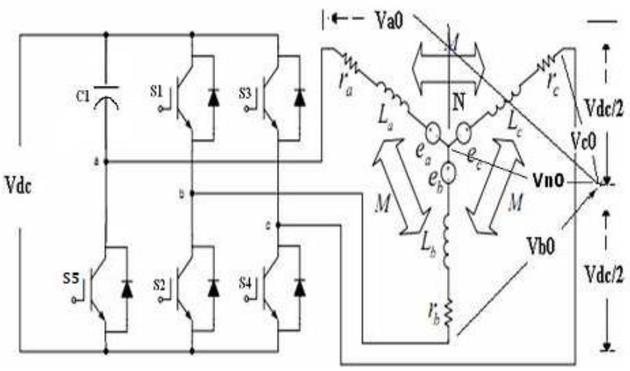

Fig 1: Inverter Circuit with BLDC Machine

I) 2π/3 ANGLE SWITCH ON MODE

The operation of Inverter in this mode is explained with the help of the waveforms shown in Fig 1. The size switches of the inverter ($Q_4 - Q_6$) operate in such a way place the input DC current I_d, symmetrically for the $2\pi/3$ angle at the center of each phase voltage wave. The angle α shown is the advance angle of current wave with respect to voltage wave. In this case, α is zero, It seems to be at any instant, two switches are ON, one in the upper group and another in the lower group. For example for instant t_1, Q_1 and Q_6 are ON when the supply voltage V_d and line current I_d are placed across line ab (phase a and phase b in series). So that I_d is positive in phase a, but negative in phase b. Then, after $\pi/3$ interval (the middle of phase a), Q_6 is turned OFF and Q_2 is turned ON, but Q_4 continues conduction for the full $2\pi/3$ angle. This switching commutates $-I_d$ it from phase b to phase c while phase a continues to carry $+I_d$ as shown. The condition pattern changes at every $\pi/3$ angle, indicates six switching modes in a full cycle. The absolute position senor indicates the switching or commutation of the device at the precise instant of the waves. It can easily be seen from Fig 1.that at any instant two phases ($2V_c$) appear in series across the inverter input. The power flow to the machine at any instant is ideally constant and is
given by $P=2V_c I_d$, which is indicated at the bottom of Fig 2. The inverter is basically operated as a rotor position sensitive electronic commutator (similar to a mechanical commutator in a DC machine).

The current sensing system (armature current) based on two LEM modules can be used in any of the three phases of the motor. The measurement of the currents in the three phases is not required. Because

I) There is no neutral connection, and hence the third phase current can be obtained from the other two

II) Despite the first reason, more than enough to justify the use of only two current sensors, there is another reason, which could justify just one current sensor. The sensing of the current is only required to get the value of the magnitude (the phase-shift and sequence is given by the position sensor).

Assuming only one current sensor, it could be possible to get information of the current I_{MAX} during 2/3 of the cycle (240º). For the other 120º, the PWM could be maintained with the same duty cycle until the next information of I_{MAX} is obtained. The one-sensor system could work well under normal balanced conditions in motor windings and inverter characteristics, and with slow dynamic operation. However, in general conditions it is safer and more accurate to have at least two current sensors, which readily give redundant information. The I_{MAX} is obtained through one phase-current sensor and through two phase current sensors. Clearly, the information of one current sensor could be used, providing that the PWM is kept with constant duty cycle during the two intervals of 60º was no information about I_{MAX} is obtained. The tuning of the current controller starts with the determination of the amplitude, frequency of the triangular carrier, and the gains of the PI control. To get a PWM signal operating at the carrier frequency, the control should be adjusted to keep the reference current moving around the reference. The Fig. 3 shows the way the stator currents are controlled, through the feedback signal I_{MAX} (t). The slopes m_1 (up) and m_2 (down) are a function of the dc link voltage, and the motor model. Therefore motor model comprises the phase inductance and the back EMF. Then, the maximum error based on a carrier e_{MAX}, will depend on the slopes m_1 and m_2, on the operating point, and the carrier frequency. This situation can be expressed mathematically, with the help of Fig. 3, as seen in

$$|m_1| = \frac{E_{pp}}{xT} = \frac{E_{pp}.f}{x} \qquad x = \frac{|m_2|}{|m_1| + |m_2|}$$

$$|m_2| = \frac{E_{pp}}{(1-x)T} = \frac{E_{pp}.f}{1-x} \qquad E_{pp} = \frac{1}{f}\left(\frac{|m_1|*|m_2|}{|m_1|+|m_2|}\right) \quad (1)$$

The term ‘x’ in equation 1 represents the fraction of the period of the carrier ‘T’, when the current is increasing. According to this equation, the term ‘x’ defines the ideal output of the PWM pattern. Then, the control parameters have to be adjusted according to the index ‘x’. E_{PP} represents the peak-to-peak error of the signal.

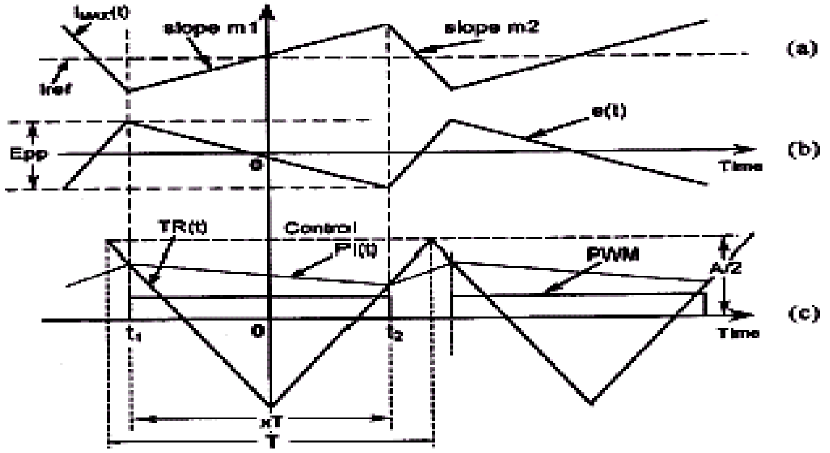

Fig 4: Ideal waveforms of (a) feedback signal I_{MAX}, (b) error signal e(t), and (c) control signals.[D1]

According to the time reference of Fig. 4, the following relations can be written:

$$\left.\begin{array}{c} (t_2 + t_1) < x \times T \\ (t_2 - t_1) = x \times T \\ |t_2| \leq |t_1| \\ e\,(t_2) + e\,(t \\ e\,(t_2) - e\,(t_1) = E_{pp} \\ e\,(t_1) = \frac{E_{pp}}{2} \end{array}\right\} \quad (2)$$

same value at t_1 and t_2, because these are intersection points that define the PWM generation

$$PI(t_1) = TR(t_1) \rightarrow K_p \times e_c(t_1) + M = -\frac{2.A}{T} \times t_1 - \frac{A}{2} \quad (3)$$

$$PI(t_2) = TR(t_2) \rightarrow K_p \times e_c(t_2) + M = \frac{2.A}{T} \times t_2 - \frac{A}{2} \quad (4)$$

With equation 5.17 and equation 5.18, K_P and M are obtained

$$K_p = \frac{\frac{2.A}{T}\cdot(t_2+t_1)}{\alpha\cdot(e(t_2)-e(t_1)} < \frac{\frac{2.A}{T}\cdot x\cdot T}{\alpha\cdot(e(t_2)-e(t_1)} \quad (5)$$

Now, when the current I_{MAX} is increasing, the error e(t) can be modeled as

$$e(t) = -m_1 \times t + n_1, \qquad \text{para } t \in [t_1, t_2] \quad (6)$$

If the rate of conversion of the magnitudes is 1:α, then the expressions of the error e_{ci} (t) becomes as shown in

$$e_c(t) = \alpha \times e(t). \quad (7)$$

On the other hand, the output of the PI control can be expressed as:

$$PI(t) = K_p \times e_c(t) + K_I \times \int_0^{t_1} e_c(t)\, x\, dt \quad (8)$$

Now, if it is assumed that the operation of the machine is stable, and operates under steady state, the integrator output is close to a constant. That means

$$M = K_I \times \int_0^{t_1} e_c(t)\, x\, dt = \text{constant} \quad (9)$$

The triangular carrier and the PI output have the equation 5.23

$$M = \frac{1}{2}\left[\frac{2A}{T}(t_2-t_1) - A - K_p\cdot\alpha\cdot(e(t_2)+e(t_1))\right] \quad (10)$$

Now, with the help of equation 5.16, 5.23, and 5.24, can be resumed as

$$K_P < \frac{1}{\alpha}\cdot\left(\frac{2\cdot A}{E_{pp}}\right)\cdot x \quad (11)$$

$$M = A\cdot\left(x-\frac{1}{2}\right) \quad (12)$$

Replacing equation 5.26 in 5.20, the value K_I of is obtained

$$K_I = \frac{A\cdot\left(x-\frac{1}{2}\right)}{\int_0^{t_1} e_c(t)\, x\, dt} = \frac{A\cdot\left(x-\frac{1}{2}\right)}{\alpha\cdot\int_0^{t_1} e(t)\, x\, dt} \quad (13)$$

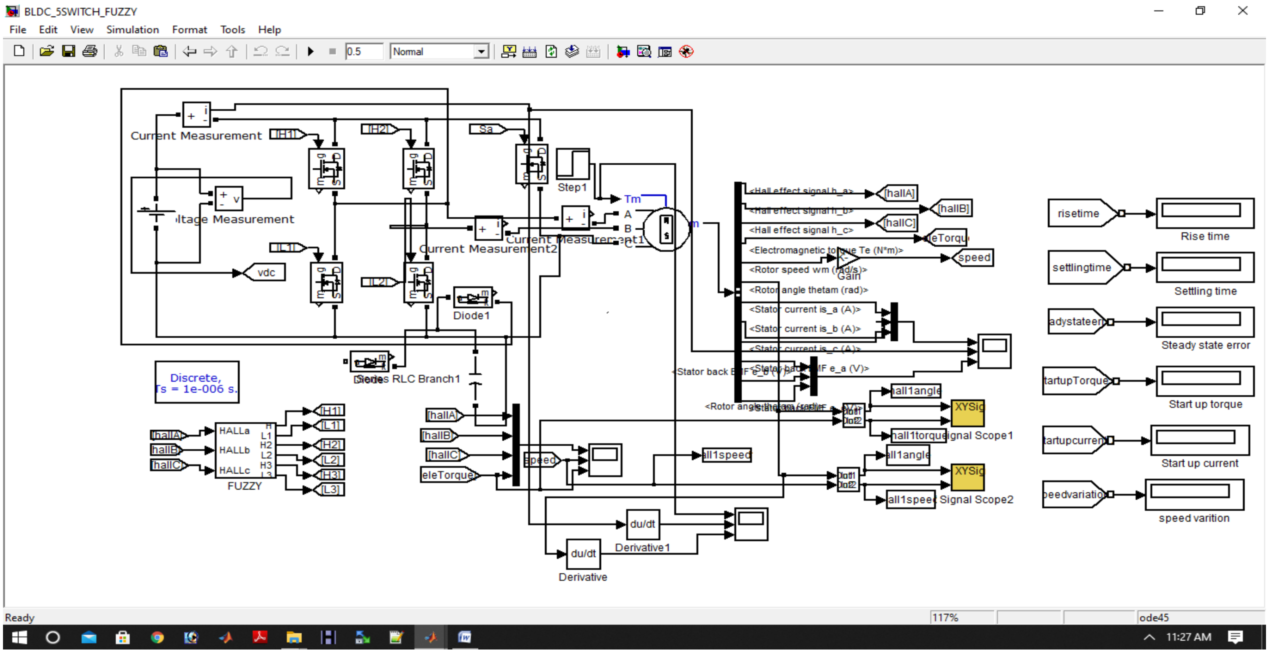

Fig 5 The Mat lab/Simulation Module of the project

III. FUZZY MODELLING

Logic of an approximate reasoning continues to grow in importance, as it provides an in expensive solution for controlling know complicate systems. Figure 5 represents the Mat lab/Simulation Module of the project. Fuzzy logic controllers are already used in appliances, washing machine, refrigerator and vacuum cleaner etc. Computer subsystems (disk drive controller, power management) consumer electronics (video, camera and battery charger) C.D. Player etc. and so on in last decade, fuzzy controllers have convert adequate attention in motion control systems. As the later possess non-linear characteristics and a precise model is most often unknown. Remote controllers are increasingly being used to control a system from a distant place due to inaccessibility of the system or for comfort reasons. In this work a fuzzy remote controllers is developed for speed control of a converter fed dc motor.

Fuzzy sets were introduced by Lofty Zadeth in 1965. They could be presented as, Let, X = {x1, x2, x3, x4, x5} crisp set called as universal set and, Let, $Y \subset x$ = {x1, x2, x3} is its crisp subset. By using the characteristic function defined as

$$\mu_Y(x) = \begin{cases} 1 \text{ if } x \in Y \\ 0, \text{ otherwise} \end{cases}$$

The subset Y can be uniquely represented by ordered pairs

$Y = \{(x_1, 1), (x_2, 1), (x_3, 0), (x_4, 0), (x_5, 1)\}$

The second member of an ordered pair (which is called the membership grade of the appropriate element) can take its value not only from the set {0, 1} but from the closed interval [0, 1] as well. By using this idea the fuzzy sets are defined as;

Let X a universal crisp set. The set of ordered pairs $Y = \{(x, \mu_Y(x)) | x \in X, \mu_Y: X\ [0, 1]\}$ is said to be the fuzzy [24] subset of X. The μ_Y: [0, 1] function is called as membership function and its value is said to be the membership grade of x. A modified format of fuzzy model proposed by Takagi and Sugeno is described by fuzzy if-then rules whose resulting parts are represented by linear equations. The following fuzzy model is If x_1 is A_{i1} . . . , x_n is A_{in} then $y_i = c_{i0} + c_{i1}x_1 + \ldots + c_{in}x_n$

Where i = 1, 2, . . ., N, N is the number of if-then rules, $c_{ik}(k = 0, 1, . . . , n)$ are the consequent parameters, y_i is the output from the i^{th} if-then rule, and A_{ik} is a fuzzy set. Given an input ($x_1, x_2 . . . x_n$), the final output of the fuzzy model is referred as follows:

$$Y = \frac{\sum_{i=1}^{N} w_i y_i}{\sum_{i=1}^{N} w_i} = \frac{\sum_{i=1}^{N} w(C_{i1}+C_{i1}T_1+\cdots+C_{i1}T_n)}{\sum_{i=1}^{N} w_i} = \frac{\sum_{i=1}^{N} \quad \sum_{i=1}^{N} wC_{ik}T_k}{\sum_{i=1}^{N} w_i} \qquad (14)$$

Where $x_0 = 1$, ω_i is the weight of the i^{th} IF-THEN rule for the input and is calculated as,

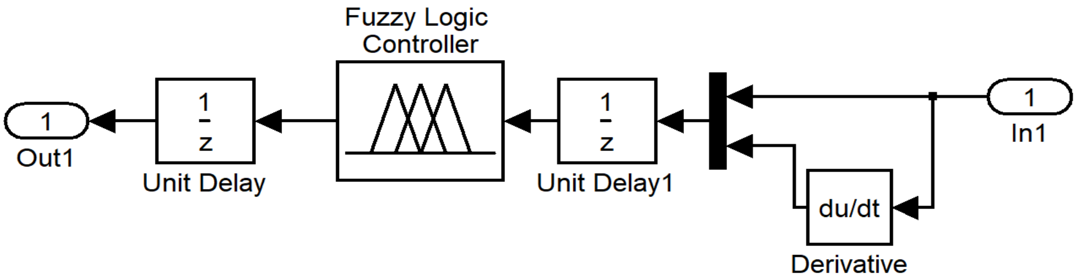

Fig 6: BLDCM fuzzy based subsystem for the Five Switch

To Takagi-Sugeno approach, the universal approximation property is proved in. In addition, a further generalization of this approach was proposed in which in the conclusion of each rule, the desired output y is given not by an explicit formula, but by a (crisp) dynamical systems [25], i.e., by a system of differential equations that determine the time derivative of the output variable as a function of the inputs and of the previous values of output. This generalization also has universal approximation property. A simplified Takagi-Sugeno fuzzy model is proposed with the following rule base.

$$\text{If } x_1 \text{ is } A_{i1} . . . , x_n \text{ is } A_{in} \text{ then } y_i = k_i(c_0 + c_1x_1 + . . . + c_nx_n) \qquad (15)$$

Where i = 1, 2. . . N, N is the number of if-then rules. From this it can be seen that the free parameters in the consequent part of the IF-THEN rules are reduced significantly in this case. The universal approximation property of this simplified T-S fuzzy model has also been proved, and successfully applied to the identification and control of nonlinear systems [26]. The advantage of solving the complex nonlinear problems by utilizing fuzzy logic methodologies is that the experience or expert’s knowledge described as a fuzzy rule base can be directly embedded into the systems for dealing with the problems. A number of improvements have been made in the aspects of enhancing the systematic design method of fuzzy logic systems [24]. In these researches, the need for effectively tuning the parameters and structure of fuzzy logic systems are increased. Many researches focus on the automatically finding the proper structure and parameters of fuzzy logic systems by using genetic algorithms evolutionary programming, and so on. But there still the problem of automatic partition of the input space for each input output variables, optimal selection of the fuzzy [24] rules needed for properly approximating the unknown nonlinear systems and to atomize the selectivity.

For the modeling of fuzzy logic a Sugeno fuzzy model has been used. The inputs given to the fuzzy model are the motor speed error and current error. The speed error is computed by the input of armature current and error in previous armature current with measured I_a. These errors are given as input to fuzzy controller, the inputs are first scaled and are changed to linguistic set which are given as input to fuzzy model. The membership functions for the error and change in error is 7 memberships.

Parameters		FUZZY
Rise time	0-700 RPM	0.004
	700-900RPM	0.003
Settling time	0-700 RPM	0.023
	700-900RPM	0.005
Steady state error	0-700 RPM	0.7%
	700-900RPM	0.7%
Start up torque	0-700 RPM	5.2N.N
	700-900RPM	2.3 N.M
Start up current	0-700 RPM	4A
	700-900RPM	2A
Speed variation	0.8%	0.7%
Power factor	0.2	0.7
DC voltage	-300	500Vdc

IV. BOOST CONVERTER

Converter a boost converter, step-up converter is a power converter with an output DC voltage greater than its input DC voltage. It is a class of switching mode power supply, called SMPS, containing at least two Semiconductors switches, a diode and a transistor, and at least one energy storage element. Switch turns on and incrementally stores energy from V1 in L. Switch turns off and this energy and additional energy from input is transferred to output. Therefore, L used as a temporary storage element filters made of inductor and capacitor combinations are often added to a converter's output to improve performance. The output voltage function for this converter is

$$V_o = \frac{V_{IN}}{1-D}$$

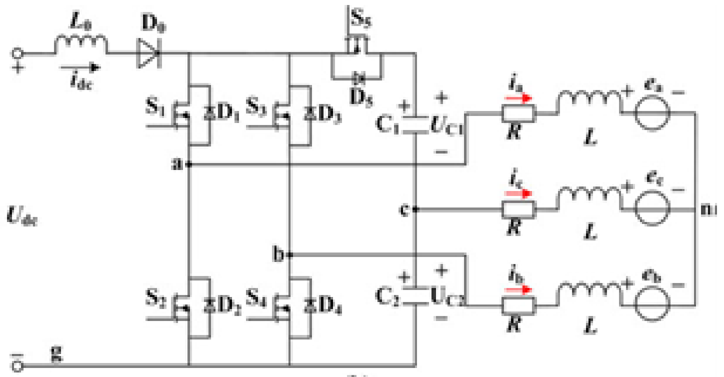

(b)

Fig 7: BLDCM drives, three-phase currents five commutating points

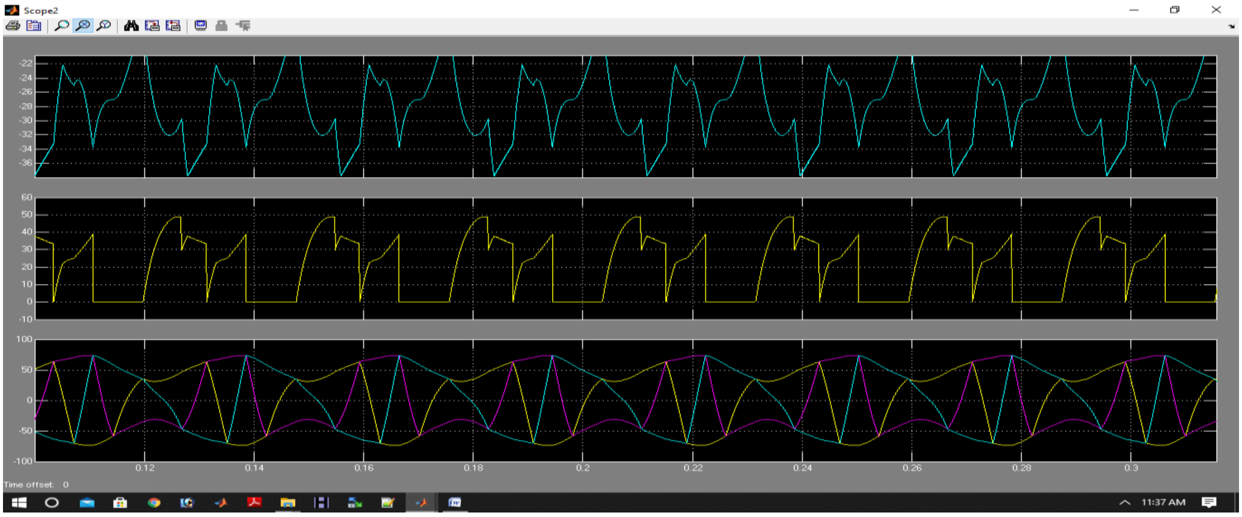

Fig 8: BLDCM five switch wave forms using Fuzzy logic method

In BLDCM drives, three-phase currents commutate in every 60° electrical degree, where the six commutating points of motor are detected by a Hall-effect position sensor. The operation of motor can be divided into six modes according to different hall values from Hall-effect position sensors. In each mode, two phases are conducting while the other is silent. Fig. 8 gives the conventional inverter and the proposed topology for BLDCM drive systems, respectively. As shown in Fig. 9, *ia*, *ib* , and *ic* are phase currents; *ea*, *eb* , and *ec* are phase back-EMF; *R* and *L* are phase resistance and inductance, respectively; *i*dc is dc link current; "*n*" is the neutral point of stator windings. The common characteristic of the two topologies is that the terminal of phase C is directly connected to the neutral point of dc link capacitors. Compared with the FSTP inverter shown in Fig. 8, a voltage boost inductance *L*0, a diode *D*0 on the side of power supply, and a mode-switching switch *S*5 on the side of dc link are added to the proposed BFSTP topology, as shown in Fig. 8. With the novel topology, the voltage across the capacitors *C*1 and *C*2 can be boosted, so the utilization of power supply voltage *U*dc is improved. It is especially suitable for the case of low power supply voltage. The function of *L*0 is to store energy when shoot-through vectors are working, where *S*1 and *S*2 (*S*3 and *S*4) in BFSTP topology are turned ON simultaneously. Then, the energy stored in inductance is transferred to capacitors on the side of dc link when *S*1 (*S*3) is turned OFF, thus boosting the voltage across capacitors. The function of *D*0 is to block energy flowing reversely from the side of dc link capacitors to the side of power supply when *S*5 is switched ON, since through boost control, the voltage across dc link capacitors is higher than power supply voltage *U*dc. *S*5 is a mode-switching switch, which is turned ON or OFF according to different operation modes of BLDCM. The fig 11 shows the power factor and the DC voltage of the converter of the five-switch with the help of fuzzy logic control. The simulation results of the figures will be observed in figures 10, 11, 12, 13.

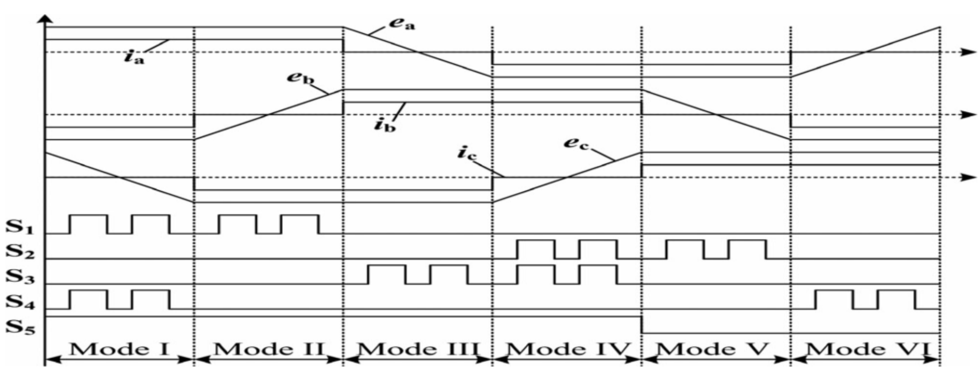

Fig.9. Relation of back-EMF, expected currents, and control signals of switches with common bipolar modulation.

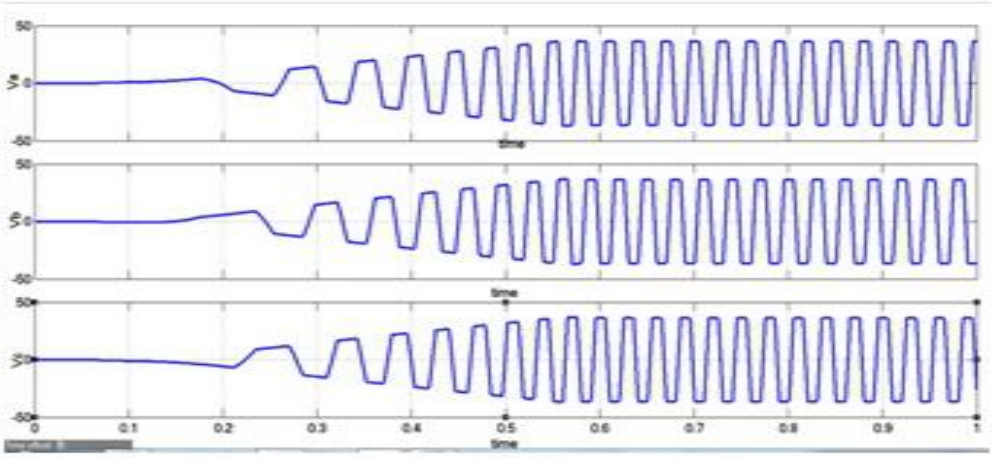

Fig 10: Stator Back EMF Ea, Eb, Ec

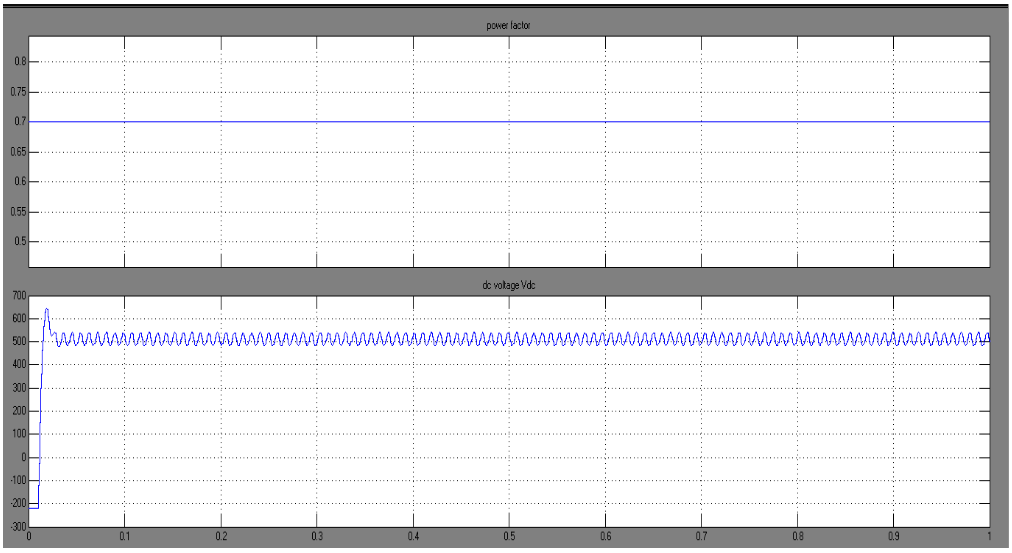

Fig 11: Power factor (PF 0.7) & dc voltage (Vdc 500)

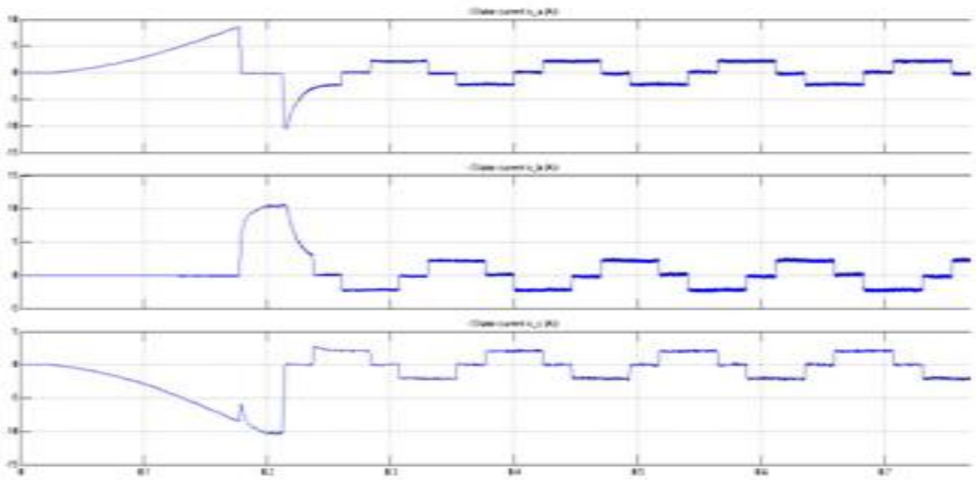

Fig 12: Stator currents fed to BLDC motor Ia, Ib, Ic

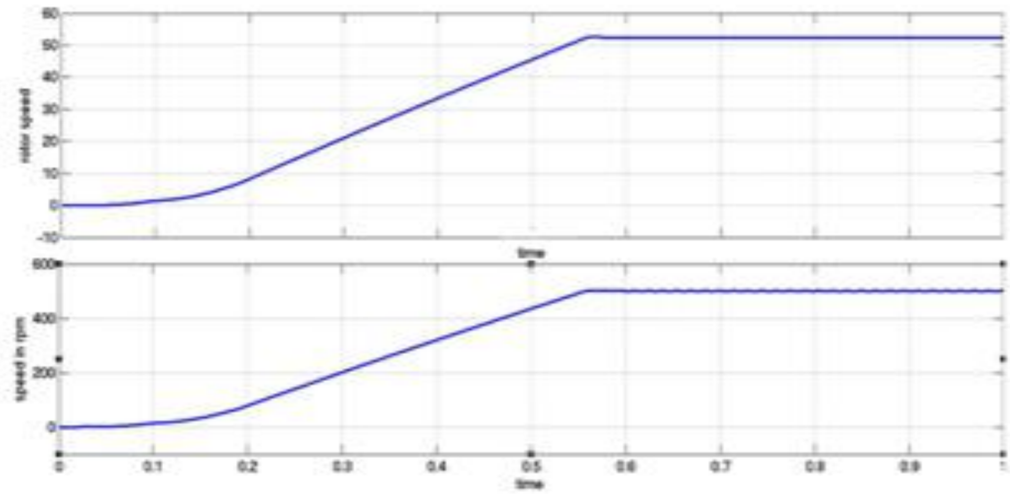

Fig 13: Rotor Speed in RPM

V. CONCLUSION

Permanent-magnet brushless dc motors is more widely used in high-performance applications because of their higher efficiency, higher torque in low-speed range, high power density ,low maintenance and less noise than other motors. In this paper closed loop speed control of BLDC motor drive with vector current controller loop is carried out with the five switch modes of operation. From the phase voltages the virtual Hall Effect signals are produced and thus applicable in five switch inverter topology. The new method is proposed for reducing the distortions using fuzzy logic control method which responds faster and smoother to reference speed change. The proposed scheme realizes two functions. First, in Modes I and IV, the negative effect of phase C back-EMF on currents is restrained and three-phase currents are controlled to be in trapezoidal waveforms. Second, through voltage boost control by inserting shoot-through vectors in Modes V and VI, the voltage across capacitors on the side of dc link is boosted, so that the utilization of power supply voltage is improved and load and speed ranges are effectively widened under low power supply voltage. Simulation results shows that current ripple and torque ripple are minimized which enhance the performance of the drive. The results also show that the dynamic performance of the motor is quite satisfactory for various loading conditions.

REFERENCES

[1] J. C. Fang,W. Z. Li, and H. T. Li, “Self-compensation of the commutation angle based on DC-link current for high-speed brushless DC motors with low inductance,” *IEEE Trans. Power Electron.*, vol. 29, no. 1, pp. 428–439, Jan. 2014.

[2] [2] J. C. Fang, H. T. Li, and B. C. Han, “Torque ripple reduction in BLDC torque motor with non ideal back EMF,” *IEEE Trans. Power Electron.*, vol. 27, no. 11, pp. 4630–4637, Nov. 2012.

[3] [3] C. L. Xia, Y. W. Xiao, T. N. Shi, and W. Chen, “Torque ripple reduction in brushless DC drives based on reference current optimization using integral variable structure control,” *IEEE Trans. Ind. Electron.*, vol. 61, no. 2, pp. 738–752, Feb. 2014.

[4] V. Bist and B. Singh, “An adjustable-speed PFC bridgeless buck–boost converter-fed BLDC motor drive,” *IEEE Trans. Ind. Electron.*, vol. 61, no. 6, pp. 2665–2677, Jun. 2014.

[5] H. Niasar, A. Vahedi, and H. Moghbelli, "A novel position Sensorless control of a four-switch, brushless DC motor drive without phase shifter," *IEEE Trans. Power Electron.*, vol. 23, no. 6, pp. 3079–3087, Nov. 2008.

[6] [13] C.-T. Lin, C.-W. Hung, and C.-W. Liu, "Position sensorless control for four-switch three-phase brushless DC motor drives," *IEEE Trans. Power Electron.*, vol. 23, no. 1, pp. 438–444, Jan. 2008.

[7] [14] B.-K. Lee, T.-H. Kim, and M. Ehsani, "On the feasibility of four-switch three-phase BLDC motor drives for low cost commercial applications: Topology and control," *IEEE Trans. Power Electron.*, vol. 18, no. 1, pp. 164–172, Jan. 2003.

[8] [15] S. B. Ozturk, W. C. Alexander, and H. A. Toliyat, "Direct torque control of four-switch brushless DC motor with non-sinusoidal back EMF," *IEEE Trans. Power Electron.*, vol. 25, no. 2, pp. 263–271, Feb. 2010.

[9] [16] C. Xia, Z. Li, and T. Shi, "A control strategy for four-switch three-phase brushless DC motor using single current sensor," *IEEE Trans. Ind. Electron.*, vol. 56, no. 6, pp. 2058–2066, Jun. 2009.

[10] [17] C. L. Xia, Y. W. Xiao, T. N. Shi, and W. Chen, "Three effective vectors based current control scheme for four-switch three-phase trapezoidal brushless DC motor," *IET Electr. Power Appl.*, vol. 7, no. 7, pp. 566– 574, May 2013.

[11] Changliang Xia, *IEEE*, Youwen Xiao, Tingna Shi, and Wei Chen, "Boost Three-Effective-Vector Current Control Scheme for a Brushless DC Motor with Novel Five-Switch Three-Phase Topology," IEEE *Trans. Power electronics*, vol. 29, no. 12, Dec 2014.

[12] I.J.Nagrath and D.P. Kothari "Electric Machines" TATA McGraw Hill 2nd Edition, 2001.

[13] Devendra Rai "Simulink Simulator usage manual for Brushless DC motor" Dept of E&CE NIT (Surathkal) Karnataka

[14] P.Pillay and R.Krishnan "Application Characteristics of permanent magnet synchronous and brushless DC motors for servo drives" IEEE Tran. Ind. Applicant, Vol. 27, PP. 986 – 996, Sept / Oct 1991.

[15] T.Low and M.A Jabbar, "Permanent-magnet motors for brushless operation", IEEE Trans. Ind Application, Vol. 26, PP. 124-129, Jan / Feb 1990

[16] M.H.Rashid "Power Electronics Circuit, Device and Applications" PHI Publication Ltd., 3rd Edition, 2005

[17] Samir Salama "Simulation of power electronics system using "SimuPec: The new power electronics tool box for "Simulink / MATLAB" 2004, Annual, 35th IEEE, Tran. Power Electronics specialists' conference.

[18] Dal.Y.Ohm "About commutation and current control methods for Brushless motors" 29th annual IMCSD symposium, San Jose, July 26-29, 1999.

[19] Juan.W.Dixon and Ivan A.Leal "Current control strategy for Brushless DC motors. Based on a common DC signal IEEE Trans Power Electronics, Vol. 27, No.2, March 2002

[20] J.M.D Murphy and F.G Turnbull, "Power Electronic control of AC motors" Pergamon Press, 1989.

[21] Clerc M., Kennedy J., "The particle swarm-explosion, stability, and convergence in a multidimensional complex space", IEEE Trans. Evolutionary Computation, 2002, Vol. 6, p. 58 –73.

[22] M.H.Rashid "Power Electronics Circuit, Device and Applications" PHI Publication Ltd., 3rd Edition, 2005

[23] C.C.Chan and K.T Chou, “An overview of Power Electronics in Electrical vehicles” IEEE Trans. Ind. Electron. Vol. 44, PP. 3-13, Feb-1997

[24] Allaoua B., Abderrahmani A., Gasbaoui B., Nasri A., “The Efficiency of Particle Swarm Optimization Applied on Fuzzy Logic DC Motor Speed Control”, SERBIAN JOURNAL OF ELECTRICAL ENGINEERING, Vol. 5, No. 2, Nov. 2008, p. 247 – 262.

[25] Parthasarathy, K., & Narendra, K., “Identification and control of dynamical systems using neural networks”, IEEE Transactions on Neural Networks, volume-1 , March 1990, 2001,4-27.

[26] Zilkova, J., Timko, J., & Girovsky, P.,“Nonlinear System Control Using Neural Networks”. Acta Polytechnica Hungarica, Vol.3; No.4 , 2006, 85-94.